Interaction of high inertia spreading films

Roisman I. V.[1], Prunet-Foch B.[2], Tropea C.[1], Vignes-Adler M.[2]

1 Technische Universität Darmstadt, Darmstadt, Germany
2 Université de Marne la Vallée, Marne la Vallée Cedex 2, France

The present experimental and theoretical work investigates the interaction of high inertia films produced by the simultaneous impact of two drops onto a dry, rigid, partially-wettable substrate. Such interaction leads to the creation of uprising liquid sheets followed by a splash. The theoretical model describes the motion of the interaction line on the substrate, the shape of the sheet and the propagation of the rim formed at the edge of the sheet. This study has the potential importance for the modelling of dense polydisperse sprays.

1. Introduction

High inertia spreading films are typical of a high Reynolds and high Weber number drop impacts ($\mathrm{Re} = \rho U_0 D_0 / \mu >> 1$, $\mathrm{We} = \rho U_0^2 D_0 / \sigma >> 1$ where ρ, σ, μ are the density, surface tension and the viscosity, D_0 and U_0 are the drop diameter and impact velocity). In the case of a drop impact onto a dry surface such a high inertia film (lamella) is bounded by a rim, created due to capillary forces [1]. Such rims also appear at the edge of free liquid sheets studied in [2], [3].

One unique feature of drop impact onto a liquid film is the interaction of the flow produced by drop impact with the outer liquid film on the substrate. This interaction leads to the creation of uprising liquid sheets, as observed in the experiments of single drop impact onto a steady uniform film [4], of the impact of the train of drops [5], and of the interaction of two drops impacting simultaneously onto a dry substrate [6]. Accounting for the interaction of wall films is especially important for describing the impingement of a dense polydisperse spray, where most conventional spray impact models based on the simple superposition of single drop impacts yield unsatisfactory results [7]. The subject of the present work is the interaction of liquid flows produced by the simultaneous impact of two Newtonian drops onto a dry, partially wettable rigid substrate.

The theoretical description of the interaction of two drops upon impact is based on recent progress in the understanding the single drop impact, which is described as the propagation of a rim bounding the radially expanding thin liquid film (lamella). The equations of the rim motion are obtained from the mass and momentum balance for each drop [1]. The motion of the interaction line (which is actually the base of the uprising sheet) is described using the concept of "kinematic discontinuity" proposed by [5] for the impact of a drop with a thin liquid layer. The mass, momentum and energy balance at this interaction line yield the expressions for the thickness and the velocity of the uprising sheet [8]. Then, the analytical expressions for the shape of the sheet is obtained from the ballistic trajectories of each material point [1]. The sheet is bounded by a rim collecting the liquid from the sheet [3]. The motion of this rim is captured by a Taylor–type analysis [2].

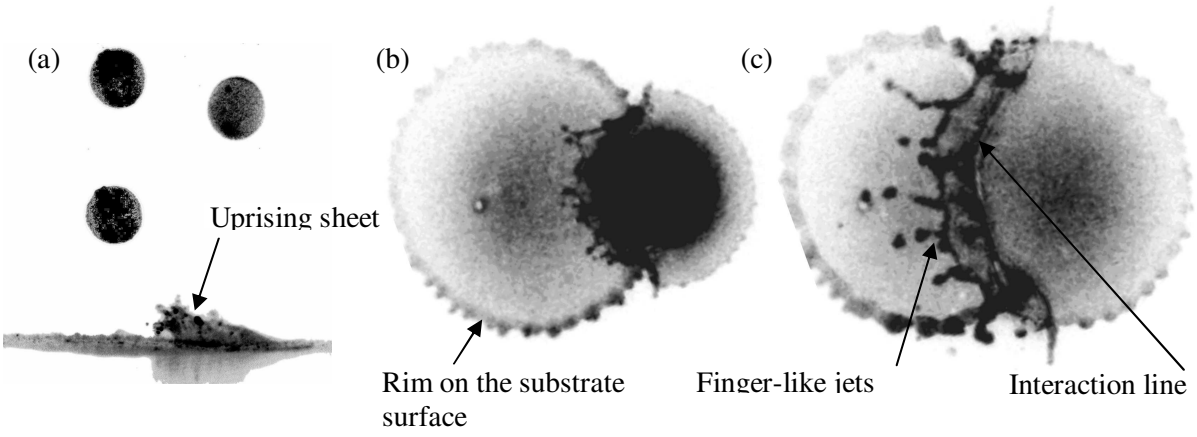

Fig. 1: Image of two impacting drops. (a) - (b) side view and top view 1.96 ms after the first drop impact; (c) top view 2.95 ms later.

2. Experiments

The simultaneous impact of two water drops on a partially wettable dry substrate was studied. The initial diameters were D_0=2.5±0.1 mm and the impact velocity U_0=3.5±0.1 m/s. The distance Δx between the points of impact and the time interval Δt between the impact instants were precisely controlled and varied. The side and the top views of the impacting and spreading drops were captured using two CCD cameras. One example of such drop interaction is displayed in Fig. 1.

As in the case of a single drop, the two drops spread and then recede due to capillary forces. Their outcome depends on the parameters characterizing their interaction, Δx and Δt. Whatever the values of Δx and Δt, the interaction of the spreading drops lead to the formation of an inclined uprising sheet on the interaction line, but not on the dry side. This sheet is bounded by a rim, formed at its edge by capillary forces. In some cases the rim becomes unstable and breaks up, leading to the creation of finger-like jets and secondary drops. It is important to note that an impacting single drop does not splash under the same

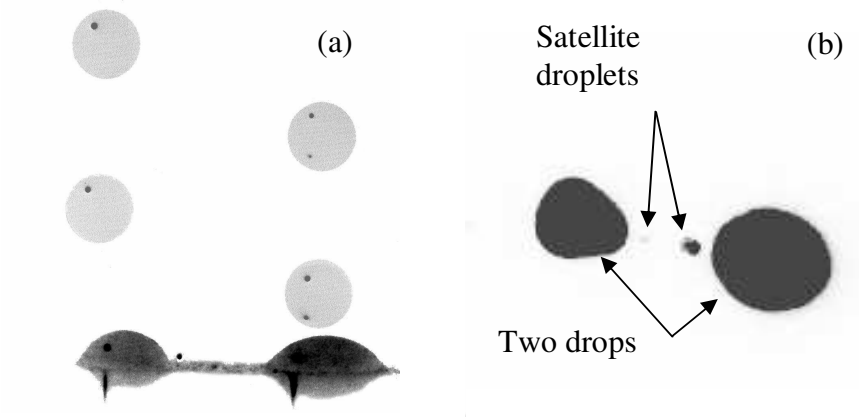

Fig. 2. The final result of the drop impact onto a dry substrate and collision. The impact parameters are the same as in Fig. 1. (a) Side views at four different times, fourth exposure at t = 1 s, (b) top view, t = 1 s.

experimental conditions. This indicates the significance of the drop interaction on the outcome of spray impact. In Fig. 2 the final result of drop impact is shown. Two separate drops on the substrate and two satellite droplets are produced during the separation.

3. Theoretical modelling

The theoretical model of the interaction of two impacting drops on a substrate includes

- hydrodynamics of a liquid film on a substrate
- description of a single drop impact
- interaction of two films on a wall leading to the formation of an uprising liquid sheet
- propagation of a free liquid sheet
- creation and motion of a rim by capillary forces

Motion of a liquid film on a plane substrate

The theory of the flow in the film is given in [5] for the axisymmetric case and generalized in [8] for the case of a two-dimensional plane film. The continuity equation of the film can be given in the following form:

$$\frac{\mathrm{D}h}{\mathrm{D}t} + h(\nabla \bullet \boldsymbol{V}) = 0 \qquad (1)$$

where h is the film thickness, $\boldsymbol{V}$ is the average velocity vector over the film thickness and parallel to the wall, ∇ is the two-dimensional gradient operator in the plane parallel to the wall, D/Dt is the material time derivative.

If the gradient of the film thickness is small ($|\nabla h| << 1$) the momentum balance equation in the plane parallel to the wall can be written in dimensionless form

$$\frac{\mathrm{D}\boldsymbol{V}}{\mathrm{D}t} = \frac{1}{We}\nabla(\nabla^2 h) \qquad (2)$$

Equation (2) and all the equations below are given in dimensionless form with D_0 and U_0 being used as the length and the velocity scales.

If the Weber number is very high (We >>1) the right-hand-side of (2) can be neglected and the general solution can be given in the Lagrangian form [8]:

$$\boldsymbol{V} = \boldsymbol{V}_0(\boldsymbol{\zeta}), \qquad \boldsymbol{x} = \boldsymbol{V}_0(\boldsymbol{\zeta})t + \boldsymbol{\zeta}, \qquad h(\boldsymbol{\zeta}) = \frac{h_0(\boldsymbol{\zeta})}{1 + (\nabla_{\boldsymbol{\zeta}} \bullet \boldsymbol{V}_0)t + \det(\nabla_{\boldsymbol{\zeta}} \boldsymbol{V}_0)t^2} \qquad (3)$$

where $\boldsymbol{x}$ is the radius vector of a material point initially located at $\boldsymbol{\zeta}$, $\boldsymbol{V}_0$ and h_0 are the initial velocity vector and the initial film thickness at the radius vector $\boldsymbol{\zeta}$, $\nabla_{\boldsymbol{\zeta}} = \partial / \partial \boldsymbol{\zeta}$ is the gradient operator at the initial instant of time.

In the case of high Reynolds numbers, a boundary layer is formed immediately after the beginning of the film motion (after the drop impact). This boundary layer is the asymptotic flow matching the outer non-viscous flow $\boldsymbol{V}$ with the boundary conditions at the wall surface. The energy loss due to the viscous dissipation in the boundary layer leads to an increase of the boundary-layer thickness δ in the flow direction. It is important to note that the boundary layer by definition cannot influence the outer solution governed by equations (1) and (2) and therefore cannot affect the spreading of the drop.

The dimensionless thickness δ can be approximated by the thickness of the boundary layer corresponding to the Stokes' first (or Rayleigh's) problem: $\delta \sim t^{1/2}\,\mathrm{Re}^{-1/2}$. At some time instant t^*, the boundary layer reaches the free surface of the film: $\delta(t = t^*) = h(t = t^*) = h^*$. This means that at times $t > t^*$ the outer solution disappears and the concept of the boundary layer can no longer be applied to the modeling of the flow. The

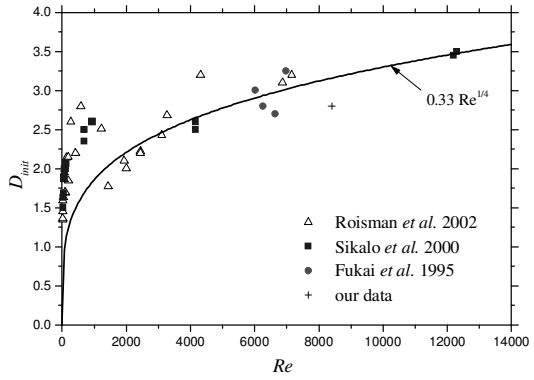

Fig. 3. Single drop impact. Dimensionless diameter of the drop at the dimensionless time instant $t = 1$. The experimental data shown are from our study, from [1], [10] and [11].

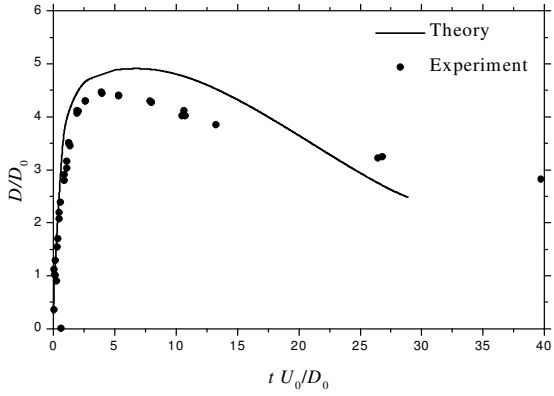

Fig. 4. Single drop impact. Temporal evolution of the drop diameter on a substrate. Comparison of the theoretical prediction with the experimental data. *We* = 387, *Re* = 8400.

viscosity influences the flow at this stage. The influence of viscosity was estimated in [9] by simply assuming a parabolic velocity profile over the film thickness. The theory predicts the asymptotic lower non-zero limit for the film thickness.

Single drop impact onto a dry wall

In [1] the drop impact process is subdivided into a number of main stages: initial drop deformation, spreading, receding, creation of a central jet.

The first stage is the initial deformation of the drop, when liquid of the drop is squeezed between the wall and the rear part of the drop, which is only slightly influenced by the impact. This squeezed liquid creates an expanding film (lamella) bounding by a rim. The approximate duration of this first stage of drop impact is $t_{init} \approx 1$. In [1] the thickness h_{init} and the diameter D_{init} of the lamella at the time instant $t = t_{init}$ are estimated from the total mass and momentum balance of the drop during the deformation stage. The distribution of the pressure produced by the drop on the substrate is determined, assuming creeping flow in the region between the wall and the rear part of the drop. The shape of the drop at the instant t_{init} is approximated by a cylinder, with the diameter obtained from the mass balance in the form:

$$3We + 5(1 - \cos\langle\theta\rangle)Re\, h_{init} = 10ReWe\, h_{init}^3 \qquad D_{init} = 2^{1/2}3^{-1/2}h_{init}^{-1/2} \tag{4}$$

It is interesting that the agreement with experiments (see [1]) is good even at high Reynolds numbers. The reason is probably in the very small volume of the considered region in comparison with the total volume of the drop. The inertia of the liquid in this region is therefore negligibly small in comparison with the total inertia of the impacting drop. The dynamic contact angle $\langle\theta\rangle$ is determined in [12] as a function of the static contact angle and the capillary number Ca_{CL} (Hoffman's law). In [1] it is determined assuming that the velocity of the contact line propagation at $t < t_{init}$ is of order of the impact velocity. The capillary number associated with the moving contact line in the stage $t < t_{init}$ is therefore $Ca_{\mathrm{CL}} \approx Ca = We / Re$.

Note however, that at very high Reynolds numbers the inertia increases and the creeping flow approximation is not longer precise. The thickness of the lamella at this time instant is determined by the boundary layer: $h_i \sim Re^{-1/2}$. The diameter of the lamella is therefore

$D_i \sim Re^{1/4}$ Data obtained in our studies, [1], [10], [11] confirm this conclusion. The best fit for the film thickness D_i shown in Fig. 3 is

$$D_i = 0.33\,\mathrm{Re}^{1/4} \qquad \text{if} \quad \mathrm{Re} > 2000 \tag{5}$$

In the spreading and receding stages of drop impact the rim bounding the expanding lamella determines the evolution of drop diameter. The mass and the momentum balance of the rim are given by

$$\frac{1}{2\pi}\frac{dW_r}{dt} = R_r h_l (V_l - V_r) \qquad \text{at } r = R_r \tag{6}$$

$$\frac{W_r}{2\pi}\frac{dV_r}{dt} = R_r\left[h_l (V_l - V_r)^2 - \frac{1-\cos\theta}{We} - \frac{6V_r \sin\theta}{Re(1-\cos\theta)}\right] \qquad \text{at } r = R_r \tag{7}$$

where r is the radial coordinate, W_r is the total volume of the rim, R_r is the radius of the centerline of the rim and V_r is its velocity, h_l is the thickness of the lamella and V_l is the velocity of the liquid in the lamella. The first term on the right-hand side of (7) represents the inertia of the liquid of the lamella entering the rim, the second term is associated with the capillary forces and wettability, the third term is the estimation for the viscous drag force. The expressions for h_l and V_l can be determined from (3) for the axisymmetric case in the same form as they were obtained in [5]:

$$V_l = r(t+\tau)^{-1}, \qquad h_l = \eta(t+\tau)^{-2}, \tag{8}$$

where τ and η are parameters determined from the analysis of the initial stage of the impact. The details can be found in [1].

It should be noted that independent of [1], the importance of the motion of the rim was also understood in [13] where the equations of motion similar to (6)-(7) were obtained.

In Fig. 4 the theoretical prediction for the evolution of the drop diameter $D = 2(R_r + a_r)$ where the rim half-thickness $a_r(W_r, R_r, \theta)$ is obtained from geometrical considerations, is compared with the experimental data for a single water drop impacting onto a dry steel plate. The agreement is rather good.

Interaction of two flows on a substrate, formation of an uprising sheet

The general case of the interaction of two films on a flat wall is considered in [8] where this phenomenon is modeled using the concept of "kinematic discontinuity" introduced in [5]. Consider two liquid films of the thickness $h_1(\boldsymbol{x},t)$ and $h_2(\boldsymbol{x},t)$ and moving on the wall with the velocities $\boldsymbol{V}_1(\boldsymbol{x},t)$ and $\boldsymbol{V}_2(\boldsymbol{x},t)$. The shape of the interaction line of these two films can be defined in parametric form as $\boldsymbol{x} = \boldsymbol{X}_B(\xi,t)$, where $\boldsymbol{x}$ is the radius vector and ξ is a parameter. If the Weber number and the Reynolds number are very high, this interaction line is actually the base of the uprising sheet. Denote $\boldsymbol{V}_B(\xi,t)$ as the velocity of the liquid in the uprising sheet at the wall. The mass, momentum and the Bernoulli equations applied to the intersection line as a control volume, with its inertia and the viscous losses as well as the capillary forces being neglected, yield (see [8] for the details)

$$\frac{\partial \boldsymbol{X}_B(\xi,t)}{\partial t} = \frac{\boldsymbol{V}_1 + \boldsymbol{V}_2}{2}, \quad \boldsymbol{V}_B = \frac{\boldsymbol{V}_1 h_1 + \boldsymbol{V}_2 h_2}{h_1 + h_2} + \left|\boldsymbol{V}_1 - \boldsymbol{V}_2\right| \frac{\sqrt{h_1 h_2}}{h_1 + h_2}\boldsymbol{e}_z \quad \text{at} \quad \boldsymbol{x} = \boldsymbol{X}_B \tag{9a,b}$$

where $\boldsymbol{e}_z$ is the base unit vector normal to the wall.

The shape $\boldsymbol{x} = \boldsymbol{X}_S(\xi, t_B, t)$ of the free sheet can be obtained assuming the ballistic trajectory of the material points in the sheet:

$$\boldsymbol{X}_S(\xi, t_B, t) = \boldsymbol{X}_B(\xi, t_B) + \boldsymbol{V}_B(\xi, t_B)(t - t_B) - \frac{(t-t_B)^2}{2Fr}\boldsymbol{e}_z \tag{10}$$

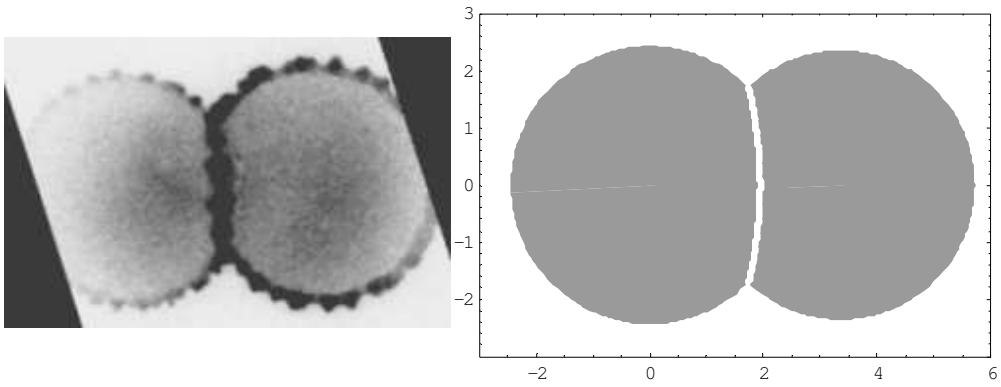

Fig. 5. Interaction of two water drops, top view: (a) experiment, (b) theoretical prediction. D_1=D_2=2.5 mm, U_1=U_2=3.36 m/s, Δt = 0.899 ms, Δx = 8.4 mm.

where $Fr = U_0^2 / g / D_0$ is the Froude number, g is gravity (the substrate is assumed horizontal). Expression (10) means that the material point belonging to the sheet is located at $\boldsymbol{x} = \boldsymbol{X}_S$ at the time instant t was ejected from the interface line on the wall $\boldsymbol{x} = \boldsymbol{X}_B$ at the time instant t_B<t.

Motion of the free rim

The motion of the rim bounding the uniform liquid sheet was studied in [2]. The velocity of the rim relative to the liquid in the sheet is

$$U_R = 2^{1/2} We^{-1/2} h_{SR}^{-1/2} \qquad (11)$$

where h_{SR} is the thickness of the sheet at the location of the rim. This expression is valid in the general case of a free curved sheet when the inertia of the rim is negligibly small and the radius of curvature of the rim centreline is much larger than the thickness of the sheet.

4. Results and discussion

The calculated shapes of the lamellas and the interface line are shown in Fig. 5, in comparison with the experimental data. The shapes of the drops are circular and not influenced by the interaction, whereas the interface line is the base of the uprising sheet.

In Fig. 6 nonsymmetrical collisions of two drops are considered. The predicted shapes of the lamellas and the position of the interaction line are shown at different time instants beginning from the first instant t_0 of the contact of two lamellas. The collision line moves towards the smaller drop. The figure-eight shape of the wetted spot is not stable. In the present study the receding of the circular part of each drop is calculated only. The creation of

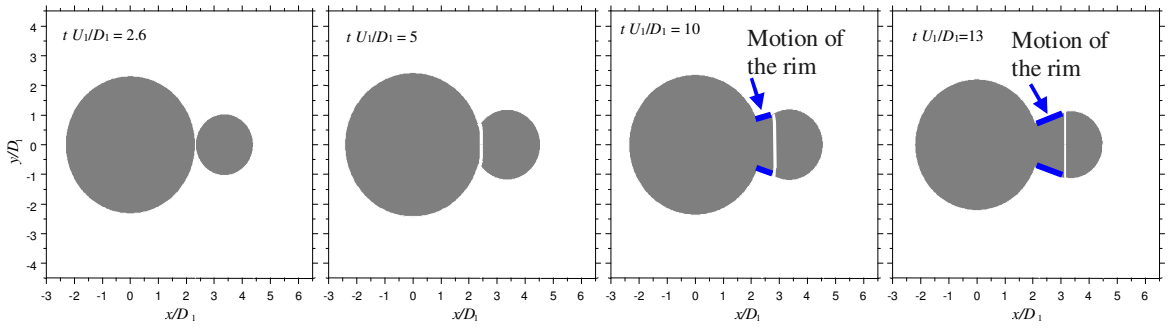

Fig. 6. The shapes of the two lamellas (gray circles) and the interface between them (white curve). D_1=2.5 mm, D_2=1.25 mm, U_1=3.36 m/s, U_2=2.38 m/s, Δt = 0.9 ms, Δx = 8.4 mm. The dimensionless time instants are: t = 2.6, 5, 10 and 13

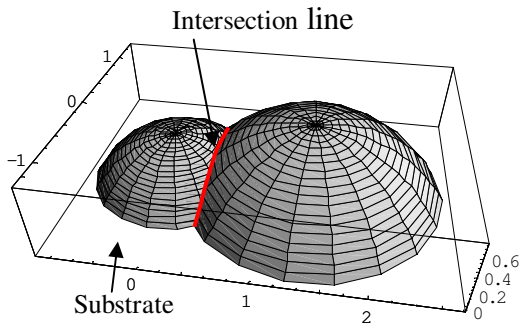

Fig. 7. Hypothetical intersection of two static drops on a substrate.

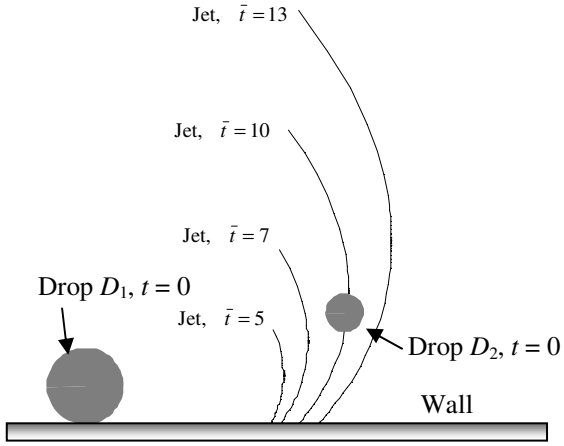

Fig. 8. Predicted shapes of the uprising jet at various time instants, as well as the positions of two impacting drops at $t = 0$. The parameters of the impact are the same as in Fig. 5.

the rim and the receding at the part connecting the two drops (in the region marked by the blue lines) are not calculated here. Actually this receding leads to further separation of the two drops, shown in Fig. 2.

Consider two liquid drops which are in contact on a substrate (see Fig. 7). In this hypothetical situation the surface curvature in the neighbourhood of the intersection line is negative and, due to capillary effects, the pressure is smaller than far from this line. This pressure difference initiates a flow towards the intersection line with the subsequent merging of two drops. Therefore, the separation of two impacting drops, as shown in Fig. 2, is caused solely by dynamic effects. The above discussion of Fig. 5 explains the mechanism of this separation.

In Fig. 8 the predicted shapes of the uprising sheet are shown at various time instants after impact. The motion of the rim is not calculated here. However the inclination of the rim towards the smaller drop can be clearly seen.

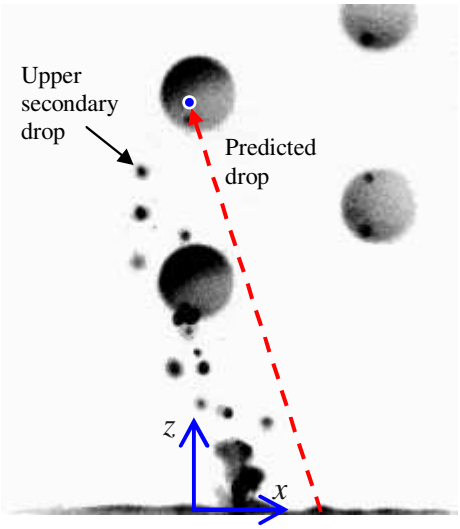

Fig. 9. Ejected droplets. Comparison with the theoretical predictions.

In Fig.9 the secondary droplets produced by the interaction can be clearly seen. The first instant of interaction, $t_0 = 1.22$, is determined from the analysis of the single drop impact (Fig. 4). The radii of the droplets at this instant are $R_1 = 1.69$, $R_2 = 0.74$. The velocities in the lamellas are also approximated from the data in Fig. 4. Assuming the thicknesses of the lamellas are approximately the same, $h_1 = h_2 = h_{init} = 0.075$, we obtain with the help of (9b) the sheet velocity $\boldsymbol{V_B} = -0.34\boldsymbol{e}_x + 1.08\boldsymbol{e}_z$. The absolute velocity of the rim elevation is less than $|\boldsymbol{V_B}|$, the relative velocity $U_R = 0.19$ is defined in (11). Assuming that the first droplets are created at the instant t_0 and ejected with the rim velocity, the location of the drop at the time instant

$t = 7.3$ corresponding to the image in Fig. 8 is $\boldsymbol{X}_{d0} = -1.75\boldsymbol{e}_x + 5.45\boldsymbol{e}_z$ which is indicated by the arrow. In Fig. 9 some small overprediction of the height of the drop can be explained by the fact that the time necessary for the creation of the drop after the first interaction is not taken into account. The predicted diameter of the droplet $D \approx 2h_{init} = 0.15$ (shown in Fig. 9 by a circle in the same scale as the photo image) agree rather well with the experiments. Therefore, the droplet's velocity and diameter are determined by the velocity and the size of the rim bounding the uprising sheet.

Conclusions

The interaction of two high-inertia liquid films is studied experimentally and theoretically using the example of the collision of two impacting drops on a solid substrate.

The experiments have shown that the impact outcome can be affected significantly by the drops collision. Such collisions can lead to the splash or to the separation of the two drops. Both phenomena are caused by dynamic effects in the films, which are described theoretically. The theoretical predictions agree well with the experiments.

This work was supported by a PROCOPE program of the German-French scientific exchange and cooperation of DAAD and MAE.

References

[1] Roisman I V, Rioboo R and Tropea C 2002 *Proc. R. Soc. London Ser. A* **458** 1411 – 1430.
[2] Taylor G I 1959 *Proc. R. Soc. London Ser. A* **253** 296 – 312.
[3] Rozhkov A, Prunet-Foch B, Vignes-Adler M 2002 *Phys. Fluids* **14** 3485 – 3501.
[4] Cossali G E, Coghe A. and Marengo M 1997 *Exp. Fluids* **22** 463—472.
[5] Yarin A L, Weiss D 1995 *J. Fluid Mech* **283** 141 – 173.
[6] Roisman I V, Prunet-Foch B, Tropea C and Vignes-Adler M 2002. *J. Coll. Interface Sci*. **256** 396 – 410.
[7] Tropea C, Roisman I V 2000 *Atomisation Spray* **10** 387 – 408.
[8] Roisman I V, Tropea C 2002 *J. Fluid Mech.* **472**, 373 – 397.
[9] Fedorchenko A I 2000 *Hydrodynamic and thermophysical features of impact of melting drops onto rigid surfaces* (Doctor Thesis, Novosibirsk, in Russian).
[10] Šikalo Š, Tropea C, Marengo M, Ganić E N 2000 In *Proc. Euro Conf.- Renewable technologies for sustainable development, Madeira Island, Portugal*, 26-29 June 2000.
[11] Fukai J, Shiiba Y, Yamamoto T, Miyatake O, Poulikakos D, Megaridis C M and Zhao Z 1995 *Phys. Fluids* **7**, 236-247.
[12] Kistler S F 1993 in "Wettability" J. C. Berg, Ed., p. 311. (New York, Marcel: Dekker Inc.).
[13] Fedorchenko A I 2000 *Russ. J. Eng. Thermophys* **10** 1-11.